## Author Query Form

**Book title:** **(SP422) Chemical, Physical and Temporal Evolution of Magmatic Systems**
**Author:** **C. P. Montagna et al.**
**Chapter:** **SP422-1162**

This is an Online First paper. Until book publication and page numbers are confirmed, please cite this chapter as:

C. P. Montagna, P. Papale & A. Longo [year]. Timescales of mingling in shallow magmatic reservoirs. *In*: Caricchi, L. & Blundy, J. D. (eds) *Chemical, Physical and Temporal Evolution of Magmatic Systems*. Geological Society, London, Special Publications, **422**. First published online [month] [date], [year], http://doi.org/10.1144/SP422.6

Where square bracketed text should be updated with actual dates.

The following queries have arisen during copy-editing your manuscript. Please provide an answer in the right-hand column below and on your proofs. Many thanks for your help.

| Query No. | Query | Response |
|---|---|---|
| Q1 | Please check this proof carefully for other errors because once it is published online the only further change will be the addition of page numbers. In particular, check that figures, tables and equations are correct. Also, please check your proof to ensure you have acknowledged your funding source (if applicable). | |
| Q2 | Please check that the wording describing the supplementary material is correct and as required. | |
| Q3 | We have deleted the reference to the supplementary material here as per style, ok? | |
| Q4 | Figures must be listed in the correct order in the text but here Figure 4 is listed before Figure 3, delete Figure 4 here? | |
| Q5 | Please check that your meaning here has not been changed. | |
| Q6 | We have changed ‘allows not to speculate’ to ‘removes speculation’, is this what was meant? Please clarify. | |
| Q7 | Please provide better quality artwork for Figure 2, if available. | |

# Q1 Timescales of mingling in shallow magmatic reservoirs

C. P. MONTAGNA*, P. PAPALE & A. LONGO

*Istituto Nazionale di Geofisica e Vulcanologia, Sezione di Pisa via della Faggiola 32, 56126 Pisa, Italy*

**Corresponding author (e-mail: chiara.montagna@ingv.it)*

**Abstract:** Arrival of magma from depth into shallow reservoirs has been documented as one of the possible processes leading to eruption. Magma intruding and rising to the surface interacts with the already emplaced, degassed magmas residing at shallower depths, leaving chemical signatures in the erupted products.We performed two-dimensional numerical simulations of the arrival of gas-rich magmas into shallow reservoirs. We solve the fluid dynamics for the two interacting magmas, evaluating the space–time evolution of the physical properties of the mixture.

Convection and mingling develop quickly into the chamber and feeding conduit/dyke, leading on longer timescales to a density stratification with the lighter, gas-richer magma, mixed with different proportions of the resident magma, rising to the top of the chamber due to buoyancy. Over timescales of hours, the magmas in the reservoir appear to have mingled throughout, and convective patterns become harder to identify.

Our simulations have been performed changing the geometry of the shallow reservoir and the gas content of the initial end-member magmas. Horizontally elongated magma chambers, as well as higher density contrasts between the two magmas, cause faster ascent velocities and also increase the mixing efficiency.

Q2 **Supplementary material:** Videos showing the evolution of magma composition with time in the shallow chamber for simulations 1–4 are available at www.geolsoc.org.uk/SUP00000.

One of the main processes characterizing the magmatic feeding systems at active volcanoes is the interaction between magmas of different chemical compositions. A typical scenario is that of a primitive, volatile-rich, hot magma rising from depth and intercepting on its way upwards an already established, volatile-poor, more evolved batch of stalling magma (Ewart *et al.* 1991). Indeed, the two magmas typically differ not only compositionally but also in terms of volatile content, and their temperatures can also be appreciably different. Such general scenario can have a variety of declinations, depending on the specific setting and physico-chemical characteristics of the magmatic mixtures involved. The shallow magma can be highly crystalline, a mush, that can be rejuvenated by the heat from the incoming component (Bachmann & Bergantz 2008); or, at the other end, it can still be hot and more fluidal, especially if injection episodes are frequent (Voight *et al.* 2010), giving rise to mixing and mingling phenomena (Longo *et al.* 2012*b*).

Depending on the timescales of the processes and on the thermal conditions of the magmatic system, the two magmas can interact on a purely physical basis, in which case the term 'mingling' is used to describe their mechanical mixing; or they can have a chemical exchange, by which their original compositions are modified, in which case the proper term defining the process is 'mixing' (e.g. Flinders & Clemens 1996).

In recent years, the importance of magma mixing and mingling processes has been recognized more and more widely (Perugini & Poli 2012). Mixing has been identified as one of the major processes generating the diversity of igneous rocks (e.g. Bergantz 2000), and it has often been invoked as an eruption trigger (Arienzo *et al.* 2010). Evidence of mingling and mixing has been found in eruptive products in many different settings, such as calderas (Arienzo *et al.* 2010; Druitt *et al.* 2012), basaltic shield volcanoes (Sigmarsson *et al.* 2005) and stratovolcanoes (Wiesmaier *et al.* 2013). Previous studies regarding magma mixing phenomena have mostly tackled the petrological and geochemical issues, with the aim of identifying parent magmas using compositional patterns (Moune *et al.* 2012); more recently, experimental studies have been performed in order to reproduce mixing patterns and characteristics in detail, and determine the behaviour of the different chemical species involved (Morgavi *et al.* 2013). Chaotic dynamics have been documented both in experimental and natural samples (Petrelli *et al.* 2011), and the morphology of mixing/mingling patterns has been linked to the time evolution of the feeding systems (Perugini *et al.* 2010).

*From*: Caricchi, L. & Blundy, J. D. (eds) *Chemical, Physical and Temporal Evolution of Magmatic Systems*. Geological Society, London, Special Publications, **422**, http://doi.org/10.1144/SP422.6
© 2015 The Geological Society of London. For permissions: http://www.geolsoc.org.uk/permissions.
Publishing disclaimer: www.geolsoc.org.uk/pub_ethics

This paper presents results obtained from numerical simulations of the arrival of primitive, gas-rich magma into a shallow reservoir, containing more evolved, degassed magma with a different composition. Patterns of convection and mingling emerge as a distinctive outcome of magma-injection processes, and they are effective on timescales of hours to days. The properties of the system, particularly geometry and volatile content, appreciably influence the efficiency and duration of the mechanical mixing process.

## The physical model

### *The magmatic system*

The focus of this work is the fluid dynamics of shallow magma chamber replenishment; specifically, the quantification of the mechanical mixing processes that occur between magmatic mixtures with different oxides compositions and volatile content. We refer, as an archetypal case, to the Phlegraean Fields magmatic system, where seismic imaging and attenuation tomographies have identified a huge (probably around 10 km wide) magma reservoir at a depth of around 8 km (Zollo *et al.* 2008; De Siena *et al.* 2010), while a variety of geophysical and geochemical evidence suggests that smaller (probably less than 1 $km^3$), shallower batches of magma have been forming throughout the caldera history at virtually any depth less than 9 km (Arienzo *et al.* 2010; Di Renzo *et al.* 2011). These shallow magma bodies have been identified as actively involved in past eruptions, which, at least in some cases, shortly followed the arrival of volatile-rich, less differentiated magmas from the deep feeding system (Arienzo *et al.* 2009; Fourmentraux *et al.* 2012). Chemical compositions of erupted magmas range from shoshonitic to trachytic to phonolitic; geochemical analyses on melt inclusions suggest a variety of processes contributing to this variability, such as recharge from depth, intra-chamber mixing and syn-eruptive mingling (Arienzo *et al.* 2010; Fourmentraux *et al.* 2012). The same analyses show that deep magmas are typically rich in gas, especially $CO_2$ (Mangiacapra *et al.* 2008).

To study the magmatic dynamics occurring as a consequence of a recharge event, we simplify the magmatic system retaining its most peculiar features. We model the injection of $CO_2$-rich shoshonitic magma coming from a deep reservoir into a shallower, much smaller chamber, containing more evolved and partially degassed phonolitic magma; the two chambers are connected by a dyke. Dealing with its aperture and propagation is beyond the scope of this paper, thus we assume that the magma of deep provenance is able to find a way to shallower depths (e.g. Lister & Kerr 1991).

### *The set-up*

Figure 1 shows the system domain for the numerical simulations. We assume one of the horizontal dimensions of the magmatic system to be much larger than the other, so that our domain is two-dimensional (2D). The deep chamber is elliptical, 1 km thick and 8 km wide; its top is at a depth of 8 km. The geometry of the shallow chamber has been varied, as shown in Figure 1, keeping its surface area fixed. In the elliptical cases, the semi-axes measure 400 and 800 m, respectively, while the circular chamber has a radius of 283 m.

The initial condition of the system is also shown in Figure 1. The shallow chamber hosts a differentiated, volatile-poor phonolitic magma. The volatile content varied from 0.3 wt% $CO_2$ and 2.5 wt% $H_2O$ to 0.1 wt% $CO_2$ and 1 wt% $H_2O$. In the feeding dyke and deep reservoir is a less evolved, basaltic shoshonite, containing 1 wt% $CO_2$ and 2 wt% $H_2O$. Table 1 lists the oxide content of the two magmas. Volatile partitioning between the gaseous and liquid phases is computed following Papale *et al.* (2006) as a function of composition and pressure. Pressure at time 0 consists of a depth-dependent magmastatic contribution superimposed onto the host-rock confining pressure. The interface between the two magmas, at the inlet of the shallow chamber, is gravitationally unstable, the lower magma being less dense owing to its higher gas content. To start the dynamics, the interface itself is not horizontal, but has a sinusoidal profile. The dynamics is solely driven by buoyancy, without any external forcing. Density contrasts at the interface vary for each simulated scenario as they depend both on volatile content and their partitioning between the liquid and gaseous phases. Volatile exsolution, in turn, depends on pressure, and thus on the depth at which the interface is placed, which is different for each geometry of the shallow chamber (Fig. 1). Table 2 summarizes the conditions for each of the simulation runs. Temperature differences between interacting magmas are often negligible (Sparks *et al.* 1977), particularly at Phlegraean Fields (Mangiacapra *et al.* 2008), thus the system is assumed to be isothermal. As a result, there is no need to speculate on the thermal status of the surrounding rock, thus reducing model uncertainties.

### *Mathematical formulation*

Interaction between the two magmas develops as a consequence of the initial gravitational instability at the interface. We solve numerically the 2D space–time evolution of the system, consisting of

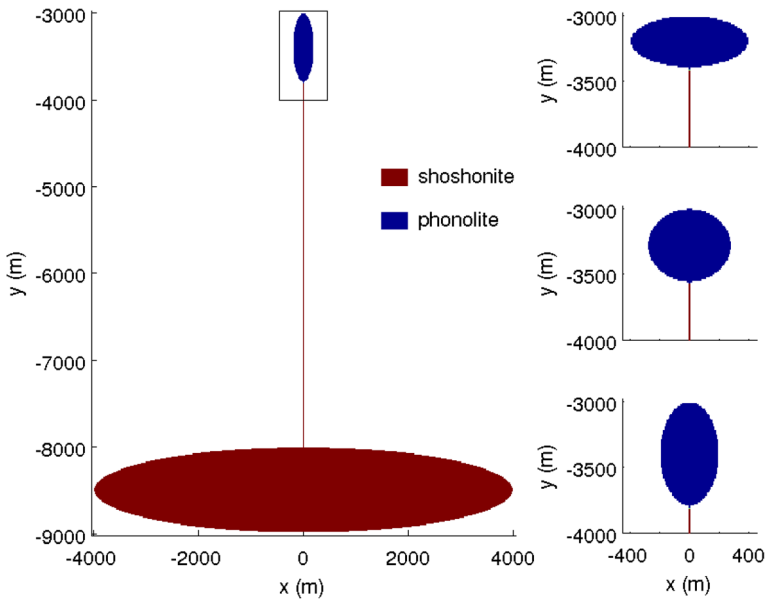


**Colour online/ colour hardcopy**

**Fig. 1.** Initial conditions for the numerical simulations of magma fluid dynamics. On the left, the whole domain is shown. On the right, the upper portion of the domain, indicated by the black rectangle, is zoomed in to show the three different geometries explored.

a mixture of two different magmatic components, each of them including a liquid (melt) and a gaseous (exsolved volatiles) fractions. The equations of motion for the mixture express conservation of mass for each component ($k = 1, 2$) and momentum for the whole mixture (Longo *et al.* 2012*a*):

$$\frac{\partial(\rho y_k)}{\partial t} + \nabla(\rho \mathbf{u} y_k) = -\nabla(\rho D_k \nabla y_k) \quad \sum_k y_k = 1 \quad (1)$$

$$\frac{\partial(\rho \mathbf{u})}{\partial t} + \mathbf{u}\nabla(\rho \mathbf{u}) = -\nabla p + \nabla\left\{\mu\left[\nabla \mathbf{u} + (\nabla \mathbf{u})^T - \frac{2}{3}\nabla \mathbf{u}\right]\right\} + \rho \mathbf{g}. \quad (2)$$

In the above, $t$ is time, $\rho$ is the mixture density, $y_k$ is the mass fraction of component $k$, $\mathbf{u}$ is the fluid velocity, $D_k$ is the $k$-th coefficient of mass diffusion, $p$ is pressure, $\mu$ is viscosity and $\mathbf{g}$ is gravity acceleration.

The magmatic mixture is considered ideal. Its density is evaluated as the weighted sum of the components' densities; for each component, density is calculated using the non-ideal Lange (1994) equation of state for the liquid phase, real gas properties and ideal mixture laws for multiphase fluids. Mixture viscosity (under the assumption of Newtonian rheology) is computed through standard rules of mixing (Reid *et al.* 1977) for one-phase mixtures and with a semi-empirical relationship (Ishii & Zuber 1979) in order to account for the effect of non-deformable gas bubbles. Liquid viscosity is modelled as in Giordano *et al.* (2008), and it depends on liquid composition and dissolved water content. The generalized Fick's law is used to describe mass diffusion (Taylor & Krishna 1993). Volatile partitioning between the gaseous and liquid phases is evaluated at every point in the space–time domain as a function of the mixture

**Table 1.** *Major oxide compositions for the two end-member magmas*

| | $SiO_2$ | $TiO_2$ | $AlO_2$ | $Fe_2O_3$ | FeO | MnO | MgO | CaO | $Na_2O$ | $K_2O$ |
|---|---|---|---|---|---|---|---|---|---|---|
| Shoshonite | 0.48 | 0.012 | 0.16 | 0.021 | 0.063 | 0.0014 | 0.10 | 0.12 | 0.028 | 0.015 |
| Phonolite | 0.54 | 0.0060 | 0.20 | 0.016 | 0.032 | 0.0014 | 0.017 | 0.068 | 0.047 | 0.079 |

**Table 2.** *List of simulations and their initial conditions; start time of the convective dynamics*

| Simulation | $CO_2$ shoshonite (wt%) | $CO_2$ phonolite (wt%) | $H_2O$ shoshonite (wt%) | $H_2O$ phonolite (wt%) | Geometry of the shallow chamber | Density contrast at initial interface (kg $m^{-3}$) | First plume (s) |
|---|---|---|---|---|---|---|---|
| 1 | 1 | 0.3 | 2 | 2.5 | Horizontal | 30 | 10 |
| 2 | 1 | 0.3 | 2 | 2.5 | Vertical | 20 | 330 |
| 3 | 1 | 0.3 | 2 | 2.5 | Circular | 25 | 220 |
| 4 | 1 | 0.1 | 2 | 1 | Horizontal | 120 | 10 |
| 5 | 1 | 0.1 | 2 | 1 | Vertical | 100 | 100 |

composition and pressure, as in Papale *et al.* (2006). All of the physical properties of the two magmas are evaluated at every point in the space–time domain depending on the local conditions of pressure, velocity and mass fractions, which are the unknowns in equations (1) and (2). The equations are solved numerically using GALES, a finite-element C++ code specifically designed for volcanic fluid dynamics (Longo *et al.* 2012*a*).

## Convection and mingling

The evolution in space and time of the system is complex and presents a number of interesting features. Figure 2 summarizes the results regarding magma dynamics, showing the evolution of composition with time in the shallow chamber for the five different simulation scenarios.

The initial inverse density contrast at the contact interface between the two magmas gives rise to convective mass transfer from the deeper parts of the system to shallower depths, and vice versa. The unstable density contrast is solely due to the different volatile content of the two mixtures: the shoshonitic melt has, indeed, a higher density than the phonolitic. The role played by volatiles is crucial, and it is the exsolved gases that ultimately determine the buoyant dynamics (Ruprecht *et al.* 2008). A Rayleigh–Taylor instability develops (Chandrasekhar 2013), which acts to bring the system to gravitational equilibrium by overturning it: a mechanism similar to what has been invoked as an eruption trigger as a consequence of chamber rejuvenation (Bain *et al.* 2013). The instability develops starting from the perturbed interface, with a first plume of light material that rises into the chamber. Depending on the initial density contrast, as well as on the geometry of the shallow chamber, the initial plume starts developing at different times, as recorded in Table 2. The dynamics is strongly enhanced by higher density contrasts; geometry also plays an important role when density contrasts are similar (simulations 1–3, 4 and 5), with horizontally elongated, sill-like chambers favouring convection with respect to more dyke-like set-ups (see also Figs 2 & 4). Q4

Plumes of light magma coming from depth keep entering the shallow reservoir as discrete filaments, following irregular trajectories and showing typical convective patterns. The lighter material tends to rise into the chamber, thereby decreasing more and more its density as volatiles exsolve in the lower-pressure environments. However, the denser magmatic mixture initially residing in the chamber sinks into the feeder dyke, increasing its density by the reverse process of volatile dissolution at higher pressures. The plumes thus progressively increase their buoyancy, enhancing their expansion and acceleration. During the rise, vortexes form at the head of the plumes and subsequent plumes interact with themselves, further favouring mixing. The dynamics create complicated patterns that maximize the interaction between the two different magmatic mixtures (Petrelli *et al.* 2011). Mingling is evident for all simulated conditions both within the chamber itself and even more in the feeding dyke, and it is strongly intensified by the chaotic patterns that form as a consequence of deep magma injection.

Independent of system geometry or density contrast at the interface, mingling is very efficient in the feeding dyke, more than inside the upper chamber. Figure 2 shows that, since the very beginning of the simulations, the magma entering the chamber is already a mixture of the two initial end members, and not the pure shoshonitic composition.

As the dynamics proceed, faster for higher-density contrasts and sill-like set-ups, the gas-rich mixture tends to accumulate at the top of the chamber, thereby originating a stable density stratification that has, indeed, been demonstrated in various magmatic systems (Arienzo *et al.* 2009). The stratification is more prominent in vertically elongated, dyke-like reservoirs (Fig. 2). The density profile along the vertical direction, evaluated averaging along horizontal planes (Fig. 3), illustrates that a quasi-stable profile is reached after some hours of simulated time.

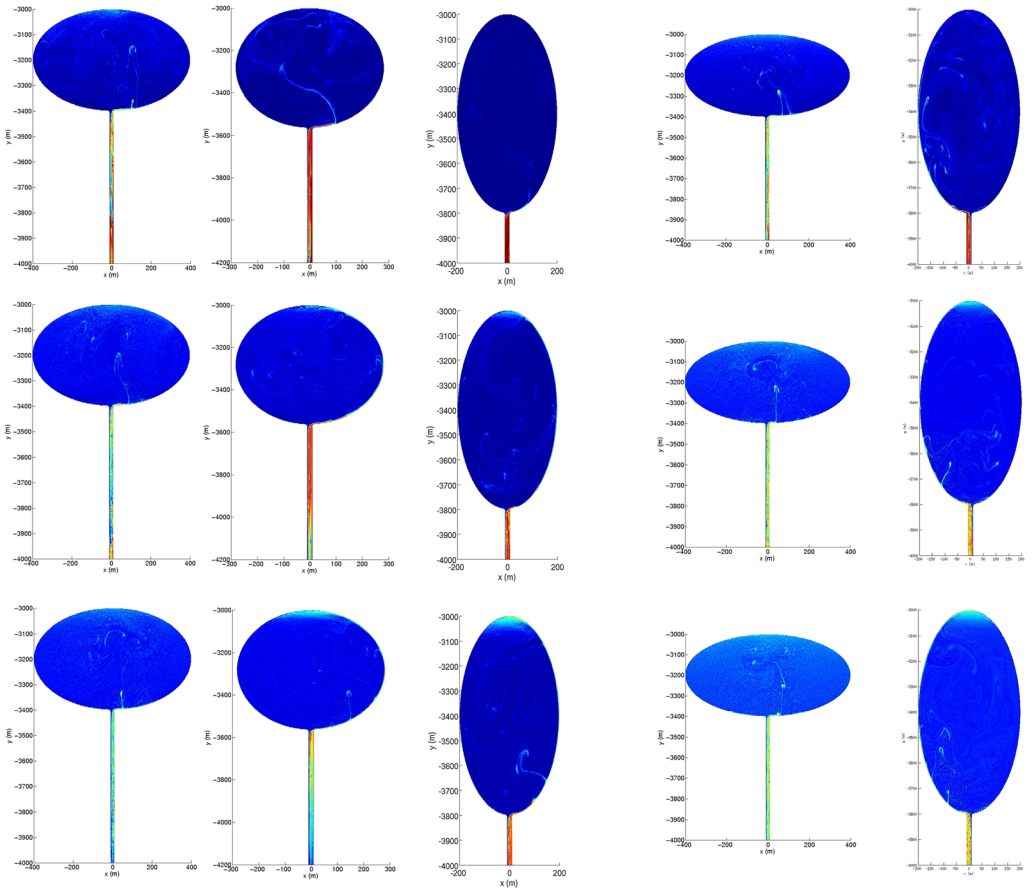

Colour online/ colour hardcopy

Q7

**Fig. 2.** Snapshots of the variation in composition with time in the shallower parts of the system for the different simulations. Columns correspond to the different simulations (simuations 1–5); rows correspond to the different times, respectively, $t = 1$, 3 and 5 h.

Q3

As time proceeds, convection slows down due to the smaller buoyancy of the incoming mixed component, and the instability proceeds asymptotically with time: the more the two end members have mingled, the less intense is convection. A time-dependent 'convection efficiency', $\eta_C$, can be

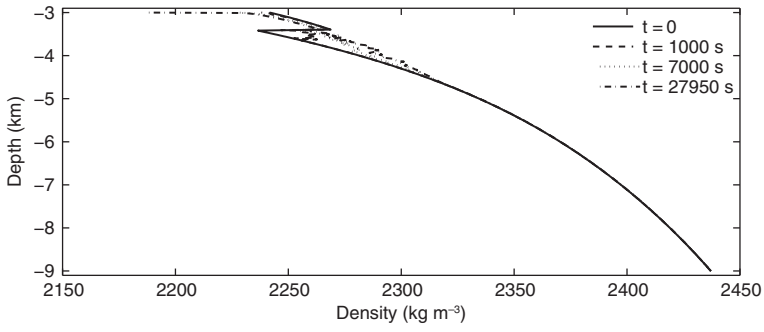


**Fig. 3.** Total mixture density averaged over horizontal planes as a function of depth for simulation 1, at different times.

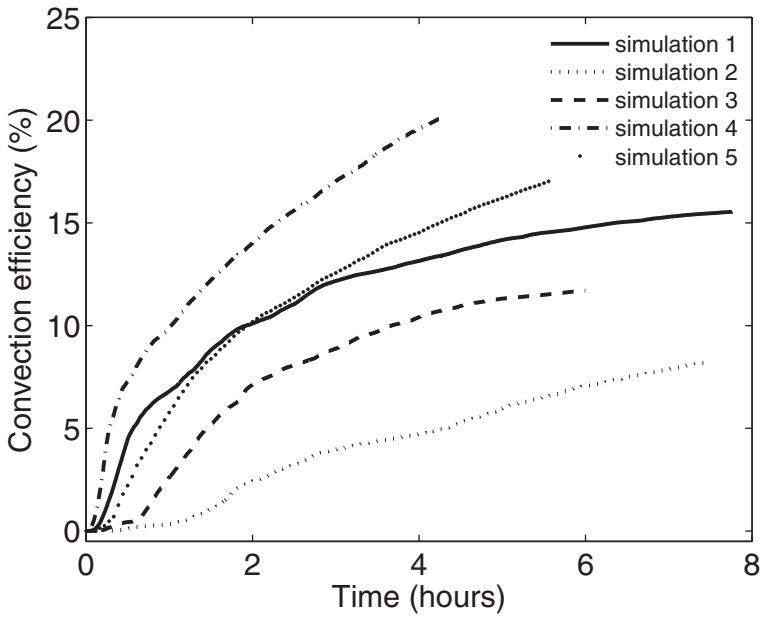


**Fig. 4.** Variation in convection efficiency with time for the different simulated scenarios in the shallow chamber. Higher density contrasts and sill-like reservoirs allow for higher convection efficiency.

defined as:

$$\eta_C = \frac{|m_R(t) - m_R(0)|}{m_R(0)}. \quad (3)$$

It represents the relative variation of the mass of the initially resident magma ($m_R$) in a certain region of the domain. Figures 4 and 5 show the time evolution of convection efficiency in the shallow chamber and in the dyke. They confirm that a higher-density contrast, as well as horizontally elongated geometries, favour convection and mixing, speeding up the processes. They also highlight that the dynamics do not start instantaneously at time 0, but at different times depending on the system conditions (Table 2). The first part of all the curves is, indeed, flat, indicating no mass exchange between the different regions of the domain.

The lower parts of the system are not involved in the system dynamics by the end of the simulated time (*c.* 6–8 h), thus we cannot comment on the evolution in those regions.

Figures 4 and 5 clearly show that mingling is very effective over relatively short timescales, of the order of hours. In the more vigorous cases, when buoyancy drives faster dynamics, more than 40% of the original end-member magmas have mingled in the feeder dyke within 4 h of the arrival of the gas-rich magma from depth. The asymptotic behaviour seems to be reached earlier in less efficient set-ups: after 4–5 h from the onset of the instability, the system seems to reach a quasi-steady state. In these cases (simulations 1–3), a much smaller proportion of the two magmas has mingled, around 10–20%.

In the final stages, the two magmas have become very efficiently mixed throughout; therefore, it is harder to identify convective patterns and rising plumes as the overall dynamics reach a quasi-steady state (Fig. 1).

## Discussion

Some important simplifying assumptions have inevitably been made to obtain the results presented above. Nonetheless, some general remarks can be extracted that might provide insights into generic magmatic processes.

One of the most important issues is that only mechanical mixing is taken into account. To this regard, it must be pointed out that at these timescales, chemical interactions between different magmas occur on length scales that are very small compared to the size of the system described here (Morgavi *et al.* 2013). This brings about a considerable technical issue if we are to describe chemical mixing in detail: the much smaller numerical grid size requested would imply a much higher computational effort, which is not sustainable within the scope of this work. The grid size for the simulations

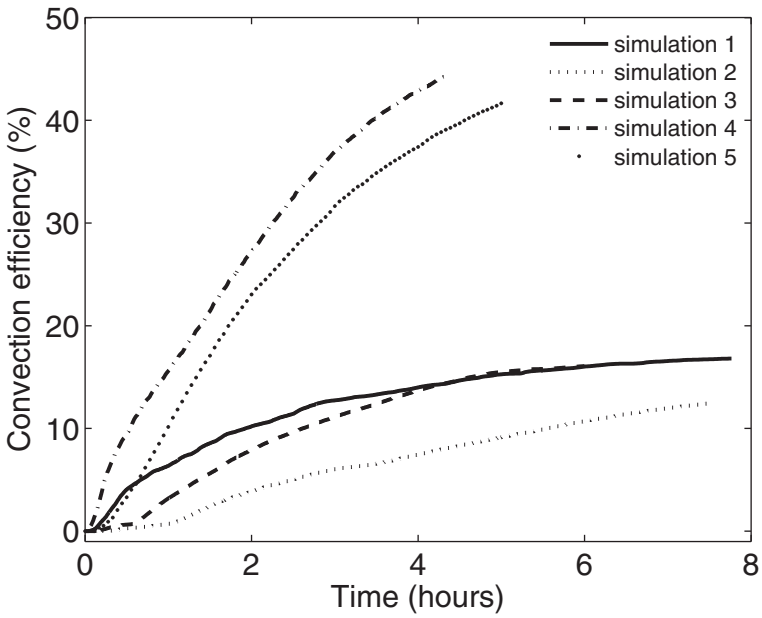


**Fig. 5.** Variation in convection efficiency with time for the different simulated scenarios in the dyke region.

described above ranges from 20 cm to 10 m depending on the dynamical behaviour of the different domain areas. This results in order $10^5$ computational elements, which is at the limit of our present computational capabilities. Neglecting chemical exchange between the two end members is acceptable at the length scales that the study is exploring in detail, which is the decameter-size scale of the overall reservoir convective dynamics. Further studies are planned to specifically address the chemical interaction occurring as mingling proceeds, to be carried out on much smaller domains. The large-scale dynamics are in very good agreement with the experimental results obtained on similar systems (Morgavi *et al.* 2013), providing good confidence in their validity.

Bi-dimensionality of the system has been assumed mainly to keep computational efforts affordable. Extension to full 3D systems should not bring about any substantial difference in the convective patterns observed, given the short timescale of our simulations and the low numerical noise. The third dimension would give rise to different dominant modes of the Rayleigh–Taylor instability (Ribe 1998), thus possibly modifying (either increasing or decreasing, depending on the amplitude of the initial perturbation) the efficiency of transport, but not substantially (Kaus & Podladchikov 2001).

The magmatic compositions used as end members for the simulations are quite similar (Table 1), and they both have quite low viscosities, even when including the effect of gas bubbles. They range from 500 Pa s in the deeper parts of the system, where most volatiles are dissolved, to 3500 Pa s in the shallow chamber for simulations 4 and 5 where the volatile content is higher and, thus, more bubbles form in the upper region of the domain. As stated in the earlier subsection on 'The magmatic system', these conditions apply to typical Phlegraean Fields eruptions (Mangiacapra *et al.* 2008). Other volcanic settings show mingling and mixing between magmas that have very different compositions, often involving rhyolites that are also characterized by much higher viscosities (Morgavi *et al.* 2013) and resulting in a higher viscosity contrast between the two magmas. Viscosity contrast has been demonstrated to play an important role in determining mixing efficiency; nonetheless, the main features of the dynamical processes remain the same as described here (Jellinek *et al.* 1999). The dynamics proceed slightly faster and mingling is more efficient when the viscosity contrast is not extreme, as in the cases considered in this work. For compositionally very different magmas, mixing is thus expected to be slightly slower and less efficient.

The assumption of an isothermal system stems from the specific case of Phlegraean Fields: as interacting magmas are so similar in composition, they were also found from melt-inclusion data to have very similar temperatures (Mangiacapra *et al.* 2008). Moreover, thermal exchange is expected to be very limited in the relatively short (hours) timescales

over which our simulations develop. Beyond the specific case of Phlegraean Fields, temperature differences between magmas involved in convection and mixing have often been found to be smaller than 10% (Sparks *et al.* 1977). The thermal state of the shallowly emplaced magma does play an important role (see the introduction to this paper) in determining the overall dynamics of the system. If it is much cooler (hundreds of K) than the intruding component, and thus largely crystallized, the dynamics would develop in completely different ways (Bain *et al.* 2013): the dyke could rise through the crystal mush and spread out on top of it, causing a gravitational instability as it degasses, and slowly reheating the underlying material. Nonetheless, such a scenario could still possibly cause, over much longer timescales (years to tens of years), buoyant mixing and overturn (Bachmann & Bergantz 2008; Druitt *et al.* 2012). The isothermal assumption reduces the computational challenges, and removes speculation on the thermal status of the rock surrounding the magmatic system.

As mentioned in the introduction, the issues related to dyke propagation and injection are not dealt with in detail. A propagating dyke is characterized by a relatively low (order of $10^6$ Pa) magma overpressurization at the tip (Lister 1990), which could act as a trigger for gravitational instability as it intercepts a magmatic body (Eichelberger & Izbekov 2000), giving rise to the buoyant dynamics described here. Short trial simulations with an overpressure imposed to the rising magma show no substantial difference in terms of the evolution of the system, as described here. The destabilizing interface perturbation acting as a trigger has a wavelength of 40 m, double the thickness of the dyke, and an arbitrary amplitude of 6 m. This configuration aims at reproducing the tip of a propagating dyke. Trial simulations performed with a flat interface show that the system becomes destabilized numerically, but takes much longer. As the focus of our discussion is on how magma chamber properties (specifically, geometry and volatile content) affect the dynamical evolution, the trigger mechanism has been kept as simple and effective as possible.

Field and geophysical observations do not provide unique constraints (Woo & Kilburn 2010) on the possible thickness of the intruding dyke. It has been set to 20 m in order to avoid issues with freezing (Rubin 1993). Apart from issues with closing, a much smaller dyke (an order of magnitude) would have drastically reduced the efficiency of transport owing to the highly increased viscous resistance from the walls, where a no-slip boundary condition is imposed.

Notably, the results obtained in this work are in remarkable agreement with previous field and experimental studies on magma mingling and mixing (Petrelli *et al.* 2011; Morgavi *et al.* 2013), both in terms of the chaotic features of the convective dynamics and the timescales for the mingling process, specifically at Phlegraean Fields (Perugini *et al.* 2010). The strength of the study presented here is that, contrary to what can be achieved in the field and laboratory, the large-scale characteristics of the natural system can be retained, thus extending and consolidating the value of the results obtained on smaller samples.

## Concluding remarks

The arrival of fresh magma into an already emplaced reservoir and the consequent internal dynamics have often been invoked as possible eruption triggers, especially at Phlegraean Fields (Arienzo *et al.* 2010). The results presented in this work clearly show that the timescales for mechanical mixing processes to be effective in magmatic reservoirs can be relatively short, of the order of hours. This is consistent with what has been observed from the analyses of erupted products (Fourmentraux *et al.* 2012), as well as from experiments on diffusive fractionation (Perugini *et al.* 2010), and opens up a completely new perspective in terms of eruption timings. Indications of mixing in erupted products suggest that recharge events can occur within a very short time frame from eruption, otherwise the evidence would be wiped out by the efficient mixing process.

Longo *et al.* (2012*b*) have shown that convective mingling dynamics in magmatic reservoirs is associated with ultra-long-period seismic signals, characterized by frequencies in the range $10^{-2}$–$10^{-4}$ Hz. Given the short timescales over which the aforementioned processes can be effective and lead to eruption, it would be beneficial to be able to routinely detect such signals for eruption forecasting and mitigation actions. This is especially true for long-dormant volcanoes such as Phlegraean Fields, one of the highest-risk volcanic areas in the world given the large population living within the caldera borders (Arienzo *et al.* 2010), for which there is still no widely accepted means of discriminating the precursors of an impending eruption (Druitt *et al.* 2012).

This work has received funds from the European Union's Seventh Programme for research, technological development and demonstration under grant agreement numbers 282769 VUELCO and 308665 MED-SUV, and from the Italian DPC-INGV V2 project.

## References

Arienzo, I., Civetta, L., Heumann, A., Woerner, G. & Orsi, G. 2009. Isotopic evidence for open system

processes within the Campanian Ignimbrite (Campi Flegrei – Italy) magma chamber. *Bulletin of Volcanology*, **71**, 285–300.

Arienzo, I., Moretti, R., Civetta, L., Orsi, G. & Papale, P. 2010. The feeding system of Agnano – Monte Spina eruption (Campi Flegrei, Italy): dragging the past into present activity and future scenarios. *Chemical Geology*, **270**, 135–147.

Bachmann, O. & Bergantz, G. W. 2008. The magma reservoirs that feed supereruptions. *Elements*, **4**, 17–21.

Bain, A. A., Jellinek, A. M. & Wiebe, R. A. 2013. Quantitative field constraints on the dynamics of silicic magma chamber rejuvenation and overturn. *Contributions to Mineralogy and Petrology*, **165**, 1275–1294, http://doi.org/10.1007/s00410-013-0858-5

Bergantz, G. W. 2000. On the dynamics of magma mixing by reintrusion: implications for pluton assembly processes. *Journal of Structural Geology*, **22**, 1297–1309.

Chandrasekhar, S. 2013. *Hydrodynamic and Hydromagnetic Stability*. Courier Dover Publications, New York.

De Siena, L., Del Pezzo, E. & Bianco, F. 2010. Seismic attenuation imaging of Campi Flegrei: evidence of gas reservoirs, hydrothermal basins, and feeding systems. *Journal of Geophysical Research*, **115**, 1–18.

Di Renzo, V., Arienzo, I., Civetta, L., D'Antonio, M., Tonarini, S., Di Vito, M. A. & Orsi, G. 2011. The magmatic feeding system of the Campi Flegrei caldera: architecture and temporal evolution. *Chemical Geology*, **281**, 227–241.

Druitt, T. H., Costa, F., Deloule, E., Dungan, M. & Scaillet, B. 2012. Decadal to monthly timescales of magma transfer and reservoir growth at a caldera volcano. *Nature*, **482**, 77–80.

Eichelberger, J. C. & Izbekov, P. E. 2000. Eruption of andesite triggered by dyke injection: contrasting cases at Karymsky Volcano, Kamchatka and Mt Katmai, Alaska. *Philosophical Transactions of the Royal Society, Series A*, **358**, 1465–1485.

Ewart, J. A., Voight, B. & Bjornsson, A. 1991. Elastic deformation models of Krafla Volcano, Iceland, for the decade 1975 through 1985. *Bulletin of Volcanology*, **53**, 436–459.

Flinders, J. & Clemens, J. D. 1996. Non-linear dynamics, chaos, complexity and enclaves in granitoid magmas. *Transactions of the Royal Society of Edinburgh: Earth Sciences*, **87**, 217–223.

Fourmentraux, C., Metrich, N., Bertagnini, A. & Rosi, M. 2012. Crystal fractionation, magma step ascent, and syn-eruptive mingling: the Averno 2 eruption (Phlegraean Fields, Italy). *Contributions to Mineralogy and Petrology*, **163**, 1121–1137.

Giordano, D., Russell, J. K. & Dingwell, D. B. 2008. Viscosity of magmatic liquids: a model. *Earth and Planetary Science Letters*, **271**, 123–134.

Ishii, M. & Zuber, N. 1979. Drag coefficient and relative velocity in bubbly, droplet or particulate flows. *AiChE Journal*, **25**, 843–855.

Jellinek, A. M., Kerr, R. C. & Griffiths, R. W. 1999. Mixing and compositional stratification produced by natural convection: 1. Experiments and their application to Earth's core and mantle. *Journal of Geophysical Research*, **104**, 7183.

Kaus, B. J. P. & Podladchikov, Y. Y. 2001. Forward and reverse modeling of the threedimensional viscous RayleighTaylor instability. *Geophysical Research Letters*, **28**, 1095–1098.

Lange, R. A. 1994. The effect of $H_2O$, $CO_2$ and F on the density and viscosity of silicate melts. *Reviews of Mineralogy*, **30**, 331–369.

Lister, J. R. 1990. Buoyancy-driven fluid fracture: similarity solutions for the horizontal and vertical propagation of fluid-filled cracks. *Journal of Fluid Mechanics*, **217**, 213–239.

Lister, J. R. & Kerr, R. C. 1991. Fluid-mechanical models of crack propagation and their application to magma transport in dykes. *Journal of Geophysical Research*, **96**, 10 049–10 077.

Longo, A., Barsanti, M., Cassioli, A. & Papale, P. 2012*a*. A finite element Galerkin/least-squares method for computation of multicomponent compressibleincompressible flows. *Computers & Fluids*, **67**, 57–71.

Longo, A., Papale, P. *et al.* 2012*b*. Magma convection and mixing dynamics as a sourceof Ultra-Long-Period oscillations. *Bulletin of Volcanology*, **74**, 873–880, http://doi.org/10.1007/s00445-011-0570-0

Mangiacapra, A., Moretti, R., Rutherford, M., Civetta, L., Orsi, G. & Papale, P. 2008. The deep magmatic system of the Campi Flegrei caldera (Italy). *Geophysical Research Letters*, **35**, L21304, http://doi.org/10.1029/2008GL035550

Morgavi, D., Perugini, D., De Campos, C. P., Ertel-Ingrisch, W. & Dingwell, D. B. 2013. Morphochemistry of patterns produced by mixing of rhyolitic and basaltic melts. *Journal of Volcanology and Geothermal Research*, **253**, 87–96.

Moune, S., Sigmarsson, O., Schiano, P., Thordarson, T. & Keiding, J. K. 2012. Melt inclusion constraints on the magma source of Eyjafjallajökull 2010 flank eruption. *Journal of Geophysical Research*, **117**, B00C07, http://doi.org/10.1029/2011 JB008718

Papale, P., Moretti, R. & Barbato, D. 2006. The compositional dependence of the saturation surface of $H_2O + CO_2$ fluids in silicate melts. *Chemical Geology*, **229**, 78–95.

Perugini, D. & Poli, G. 2012. The mixing of magmas in plutonic and volcanic environments: analogies and differences. *Lithos*, **153**, 261–277.

Perugini, D., Poli, G., Petrelli, M., Campos, C. P. & Dingwell, D. B. 2010. Time-scales of recent Phlegrean Fields eruptions inferred from the application of a diffusive fractionation model of trace elements. *Bulletin of Volcanology*, **72**, 431–447.

Petrelli, M., Perugini, D. & Poli, G. 2011. Transition to chaos and implications for time-scales of magma hybridization during mixing processes in magma chambers. *Lithos*, **125**, 211–220.

Reid, R. C., Prausnitz, J. & Sherwood, T. 1977. *The Properties of Gases and Liquids*, 3rd edn. McGraw Hill, New York.

Ribe, N. M. 1998. Spouting and planform selection in the Rayleigh–Taylor instability of miscible viscous fluids. *Journal of Fluid Mechanics*, **377**, 27–45.

Rubin, A. M. 1993. On the thermal viability of dikes leaving magma chambers. *Geophysical Research Letters*, **20**, 257–260.

Ruprecht, P., Bergantz, G. W. & Dufek, J. 2008. Modeling of gas-driven magmatic overturn: tracking of phenocryst dispersal and gathering during magma mixing. *Geochemistry, Geophysics, Geosystems*, **9**, Q07017, http://doi.org/10.1029/2008GC002022

Sigmarsson, O., Condomines, M. & Bachelery, P. 2005. Magma residence time beneath the Piton de la Fournaise Volcano, Reunion Island, from U-series disequilibria. *Earth and Planetary Science Letters*, **234**, 223–234.

Sparks, R., Sigurdsson, H. & Wilson, L. 1977. Magma mixing: a mechanism for triggering acid explosive eruptions. *Nature*, **267**, 315–318.

Taylor, R. & Krishna, R. 1993. *Multicomponent Mass Transfer*. Wiley, New York.

Voight, B., Widiwijayanti, C., Mattioli, G. S., Elsworth, D., Hidayat, D. & Strutt, M. 2010. Magma-sponge hypothesis and stratovolcanoes: case for a compressible reservoir and quasi-steady deep influx at Soufriere Hills Volcano, Montserrat. *Geophysical Research Letters*, **37**, L00E05, http://doi.org/10.1029/2009GL041732

Wiesmaier, S., Troll, V. R., Wolff, J. A. & Carracedo, J. C. 2013. Open-system processes in the differentiation of mafic magma in the Teide-Pico Viejo succession, Tenerife. *Journal of the Geological Society, London*, **170**, 557–570, http://doi.org/10.1144/jgs2012-016

Woo, J. Y. L. & Kilburn, C. R. J. 2010. Intrusion and deformation at Campi Flegrei, southern Italy: sills, dikes, and regional extension. *Journal of Geophysical Research*, **115**, B12210, http://doi.org/10.1029/2009JB006913

Zollo, A., Maercklin, N., Vassallo, M., Dello Iacono, D., Virieux, J. & Gasparini, P. 2008. Seismic reflections reveal a massive melt layer feeding Campi Flegrei caldera. *Geophysical Research Letters*, **35**, L12306, http://doi.org/10.1029/2008GL034242